



SAPIENZA
UNIVERSITÀ DI ROMA



**UNIVERSITAT
POLITÈCNICA
DE VALÈNCIA**

BACHELOR FINAL THESIS

**MEASUREMENTS OF HEAT TRANSFER IN A
MODEL BUILDING IN A WIND STREAM**

Made by
Rosa Muñoz Arnau

To obtain the title of
Aerospace Engineering

Directed by
Giovanni Paolo Romano

Made in the Department of
Mechanical and Aerospace Engineering, University La Sapienza, Roma

June 2022

Abstract

The investigation's main finding is that heat transfer from a building's surface greatly increases its overall energy consumption. Nowadays, the cost of household energy is high and it is essential to reduce heat losses to the maximum.

In order to determine how heat is transmitted in the presence of a wind stream, it is a good idea to compare the heat inside and outside of a building.

In this work, the building model is a cube completely covered and with a bulb inside. The temperature inside will be obtained with a data logger that carries four thermocouples. The outside temperature with the presence of the wind shall be assessed by an infrared camera that will take photos every second during thirty minutes.

There are three walls analyzed, three different velocities and two different positions. In total there are fifteen experiments performed.

It has been seen that the biggest change in temperature is captured from inside the sample building. From the outside, the same jump is not perceived because of the distance to which the model is located and because it is evidently farther from the heat source than the thermocouples.

Finally, all cases have been analyzed in detail and the difference in the temperatures between inside and outside the cube as well as how the position affects the temperature and also the change in speed are also studied in depth.

Acknowledgement

Words cannot express my gratitude to my professor and my project partner for their invaluable patience and feedback. I also could not have undertaken this journey without all the people who study and work in the laboratory, that any problem that might arise helped me until it was resolved.

I am also grateful to my classmates who have helped me in the most difficult moments and we have supported each other.

Thanks should also go to my friends, those who have taken my mind off studying when I have a need to disconnect from the academic and give emotional support, and those who have always trusted on me.

Lastly, I would be remiss in not mentioning my family, especially my parents and my sister. Their belief in me has kept my spirits and motivation high during this stage.

Index

I	Preface	7
1	Motivation	8
2	Introduction	9
II	Theoretical background and configuration	11
3	Heat transfer	12
4	Configuration in the wind tunnel	14
III	Results and comparisons	22
5	Parallel left face to the wind flow	23
5.1	Wind velocity of 5 m/s	23
5.2	Wind velocity of 10 m/s	25
5.3	Wind velocity of 15 m/s	26
6	Orthogonal windward	27
6.1	Wind velocity of 5 m/s	27
6.2	Wind velocity of 10 m/s	28
6.3	Wind velocity of 15 m/s	29
7	Orthogonal leeward	30
7.1	Wind velocity of 5 m/s	30
7.2	Wind velocity of 10 m/s	31
7.3	Wind velocity of 15 m/s	32
8	45 degrees windward	33
8.1	Wind velocity of 5 m/s	33
8.2	Wind velocity of 10 m/s	34
8.3	Wind velocity of 15 m/s	35
9	45 degrees leeward	36
9.1	Wind velocity of 5 m/s	36
9.2	Wind velocity of 10 m/s	37
9.3	Wind velocity of 15 m/s	38
10	Conclusions	41
	References	43
IV	Annexes	45

Index of Figures

1	Configuration of the building case	14
2	Optris PI 400i camera [13]	15
3	Location of the wires	15
4	Data logger configuration	16
5	Final configuration of the building case in the wind tunnel	16
6	Contour 45 degrees windward at 5 m/s	23
7	Contour orthogonal windward at 10 m/s	23
8	Data Logger test in the parallel left face at 5 m/s	24
9	CSV processing data in the parallel left face at 5 m/s	24
10	Data Logger test in the parallel left face at 10 m/s	25
11	CSV processing data in the parallel left face at 10 m/s	25
12	Data Logger test in the parallel left face at 15 m/s	26
13	CSV processing data in the parallel left face at 15 m/s	26
14	Data Logger test in the orthogonal windward at 5 m/s	27
15	CSV processing data in the orthogonal windward at 5 m/s	27
16	Data Logger test in the orthogonal windward at 10 m/s	28
17	CSV processing data in the orthogonal windward at 10 m/s	28
18	Data Logger test in the orthogonal windward at 15 m/s	29
19	CSV processing data in the orthogonal windward at 15 m/s	29
20	Data Logger test in the orthogonal leeward at 5 m/s	30
21	CSV processing data in the orthogonal leeward at 5 m/s	30
22	Data Logger test in the orthogonal leeward at 10 m/s	31
23	CSV processing data in the orthogonal leeward at 10 m/s	31
24	Data Logger test in the orthogonal leeward at 15 m/s	32
25	CSV processing data in the orthogonal leeward at 15 m/s	32
26	Data logger test in the 45 degrees windward at 5 m/s	33
27	CSV processing data in the 45 degrees windward at 5 m/s	33
28	Data logger test in the 45 degrees windward at 10 m/s	34
29	CSV processing data in the 45 degrees windward at 10 m/s	34
30	Data logger test in the 45 degrees windward at 15 m/s	35
31	CSV processing data in the 45 degrees windward at 15 m/s	35
32	Data logger test in the 45 degrees leeward at 5 m/s	36

33	CSV processing data in the 45 degrees leeward at 5 m/s	36
34	Data logger test in the 45 degrees leeward at 10 m/s	37
35	CSV processing data in the 45 degrees leeward at 10 m/s	37
36	Data logger test in the 45 degrees leeward at 15 m/s	38
37	CSV processing data in the 45 degrees leeward at 15 m/s	38
38	Flow field around a cube [21]	42
39	Flow field around a cube	42
40	Nusselt number changing with the velocity of the air	47
41	Reynolds number changing with the velocity of the air	47
42	CSV processing data in the half right parallel left face at 5 m/s	50
43	CSV processing data in the half right parallel left face at 10 m/s	51

Index of Tables

- 1 The cases that are going to be studied 17
- 2 Reynolds number model case 1 18
- 3 Reynolds number model case 2 18
- 4 Reynolds number cases analyzed 18
- 5 Data from the real case study 20
- 6 Reynolds and Nusselt number real case 20
- 7 Data from the model case study 20
- 8 Reynolds and Nusselt number model case 20
- 9 Comparison between Reynolds and Nusselt 21
- 10 Summary of the temperature results 39
- 11 Difference between temperature inside vs temperature outside 39
- 12 The temperature amplitude of the data logger and the camera 40
- 13 Reynolds and Nusselt number model case 46
- 14 Comparison between Reynolds and Nusselt 46
- 15 Minutes to reach the equilibrium from inside the cube 49
- 16 Minimum temperature of points from the right edge in 5 m/s 50
- 17 Minimum temperature of points from the right edge in 10 m/s 51

Part I

Preface

1 Motivation

Being an Aerospace Engineering student at the Polytechnic University of Valencia in Spain, this last year I decided to come to study at La Sapienza in Rome.

Since I was young, my parents have taught me the value of hard work, and stressed the importance of education to me. Their encouragement along with my own determination has helped me to earn some of the best grades in my high school class. These grades afforded me the ability to go to university and study aerospace engineering, which was the degree that most fascinated me.

I am responsible and eager to learn new things, I like doing things well to obtain good results. I also consider myself a person who wants a change of scenery and one that likes the ability to grow as an independent person in a place far out of my comfort zone. That is why this past year I came to study to Rome. This course has been life-changing for me. I have met many new people, people from all over the world. They have taught me to grow as a person, and to know different habits and cultures. Although Italy is quite similar to my country, there are differences and I have had to learn to develop my adult life here.

With respect to the university, it is one of the most remarkable changes that I have experienced. The method of evaluation is very different and also the format of the exams. I have always been accustomed to the most practical part of the subjects such as solving problems and doing laboratory practice every week and not having only one exam per subject. Doing oral exams and developing the theoretical part very well, it was something that I had never done and that is why the first exams were hard to pass. However, I could say that it is a method that has been useful to me to understand everything better and be able to develop the practical part more easily.

Regarding my final thesis, the professor proposed me a topic of heat transfer to work with a colleague of the master's thesis. The motivation that this project gave me was that it was a topic that I had seen during my university years but not in too much depth. I consider that it is an interesting and useful work because even if that I am analyzing a building case it could also work with numerous aeronautical applications.

I knew that this project was not going to be easy to carry out, since being something new were going to arise numerous problems. My main motivation was that it is a job that requires help and teamwork, since not having any reference was necessary to ask the professionals and also do a research for possible similar projects that have been made over the years.

To sum up, the aspect of doing the project that encouraged me the most was that it was a project of doing a lot of research and therefore reading books and papers was going to be one of the most useful things.

2 Introduction

The human species experienced a watershed moment in its evolution when the number of people living in cities surpassed that of those living in rural areas for the first time.

As a result of this influx of people from the countryside to the city, our urban landscapes are changing. As inner-city land becomes scarce, buildings are becoming more congested and higher-rise. Open green places are gradually disappearing as cities spread into the suburbs and beyond. Previously separate villages have blended into indistinguishable zones, forming massive agglomerations. As a result, it is no wonder that the climate in our cities is changing. Towns and cities are often warmer than the surrounding countryside due to the wind protection and heat retention provided by our structures [1].

This warming impact may be very welcome in certain colder countries, at least for the time being. Heating loads are lowered, gardens bloom earlier, and the requirement for winter road gritting is minimized. In other regions of the world, however, urban heat islands can pose a major health danger, especially when they occur on top of already oppressive summer heat waves. The cost of air conditioning continues to rise, dumping even more heat onto the streets and exacerbating the problem. Mortality rates rise, especially among the very young and elderly, and city life becomes less enjoyable [2].

The cost of household energy is another key issue affecting our urban lifestyle. Recent energy price increases, combined with an increasing consumer desire to be more environmentally conscious, are assisting in the mainstreaming of renewable energy technologies. Although the long-term benefits of some of these systems have yet to be established, the feel good factor of generating your own free energy has swept the industry [3].

Incorporating such renewable technology into the urban fabric poses its own set of issues; wind speeds in towns and cities are often lower than in open areas, making precise placement of home wind turbines crucial. Solar photovoltaic panels, for example, require full sunlight to generate optimum output, but they also benefit from a cooling breeze to reduce operational temperature and so increase conversion efficiency. All of these are concerns that consumers, manufacturers, and researchers are only now starting to grapple with. These are only a few of the many factors that have an impact on our urban landscapes today [1].

Wind pressures on buildings are influenced by a variety of factors, such as balconies and the roughness of the building envelope. The influence of the building envelope configuration on wind loads on cladding and structural elements of a building must be determined in order to identify any necessary changes to wind codes of practice and design standards, as well as to investigate the possibility of simplifying wind tunnel building models if the simulation of architectural details appears to be insignificant to the measured wind pressures [1].

For rational design of glass and cladding used on structures, wind-induced local stresses projected to operate on the building envelope during its lifetime are necessary. The popularity of tall structures with significant expanses of glass and lightweight cladding has raised the importance of this need in recent years. The turbulence in the wind flow approaching the building, as well as flow disturbances created by appurtenances such as surface components, balconies, or the texture of the building materials, cause pressure fluctuations on wall surfaces (uniform roughness). Because of the random character of the oncoming flow, predicting wind loads on buildings is challenging in general; however, it becomes significantly more complicated when appurtenances are included [4].

The importance of not getting air into the building is vital. As seen before, the cost of household energy is high and therefore it is necessary that all the walls are covered so that the heat inside is not lost and therefore there are no large losses of energy. This is an important characteristic that has to be taken into account.

That is why analyzing the heat that is seen from outside the building case and the heat inside it is a good analysis to see the transmission of heat in the presence of a wind stream.

Part II

**Theoretical background and
configuration**

3 Heat transfer

Convective heat transfer at exterior building surfaces is important for a variety of architectural and urban engineering applications. The turbulent convective heat fluxes from building surfaces and roadways determine the outdoor thermal climate and building cooling load in urban locations [5].

The core of the investigation is that heat transfer from a building's surface contributes significantly to its overall energy usage [6].

Heat transmission occurs at the exterior surfaces of buildings through convection and radiation processes [7]. The rate of convective heat exchange between the building envelope's surface and the surrounding air is determined by the following factors [8]:

- The temperature difference between the surface and the wind stream
- The speed and direction of any wind-driven air movement over the building
- The shape and roughness of the building surface

However, radiation heat loss is a function of surface temperature and emissivity. The ability of an object to emit infrared energy is measured by its emissivity. The amount of energy released reveals the object's temperature. It goes from 0 (a polished mirror) to 1.0 (blackbody) [9]. Because of the range of circumstances that might exist across the surface of any given building, reliable estimation of thermal energy loss from a building is challenging [7].

The short wave solar radiation input to the building's exterior surface during the day, as well as the net long wave radiation exchange at the external surface, make up radiant heat transfer. The magnitude of the outgoing long wave radiation released from the surface and the incoming long wave radiation impinge on the surface determine the net long wave radiation [6].

$$q_1 = q_{1,in} - q_{1,out} \tag{1}$$

Moreover, convection is a method of transferring heat energy through the air by conduction and mass transport. Besides, conduction is used to transport heat from the building to the immediately nearby immobile air layer. The energy is then transmitted from higher-temperature parts to lower-temperature regions via movements within the air itself [8]. Natural convection and forced convection are the two types of convective heat transfer [6].

Natural convection occurs when the movement of a neighboring air layer is caused by natural buoyancy forces caused by a change in the density of the air near the surface. In the context of forced convection, it refers to a situation in which a large applied air motion prevails over the natural component [8]. In essence, pressure decreases when fluid inside or close to the heat source and heat sink becomes hotter than the surrounding air. Less pressure means more buoyancy because gravity exists here on Earth. The hotter air moves upward and away from the source of gravity as a result of this pressure difference. The colder fluid then fills the space where the hot air was leaving, creating an upward and then inward flow [10].

Despite the fact that forced convection heat exchange is generally dominating at the building envelope's external surface, this is not always the case. The building surfaces reach temperatures well above the nearby air temperature during periods of strong incident solar radiation, resulting in a significant natural convective component [8].

Regarding the flow, laminar and turbulent flow are two types of flow that exist within the realms of both natural and forced convection. The kind of flow in an air stream is determined by the air's velocity, the

roughness of the surface it passes through, and, to a lesser extent, the air's viscosity [8]. The flow is going to be considered turbulent when Reynolds number is between 5×10^5 and 1×10^7 [11].

To a greater or lesser extent, all surfaces within an air stream have a boundary layer. Both hydrodynamic and thermal boundary layers exist in the air next to the building surface. In the first case, the hydrodynamic layer, the air layer is stationary at the building surface, with the full velocity of the air achieved at various distances from the surface. The hydrodynamic boundary layer is a transition zone where the air stream velocity increases with distance from the surface [8].

In the case of the thermal boundary layer, a temperature gradient exists perpendicular to the wall when air passes over a building surface that is at a different temperature. At the interface, the temperature of the air achieves its maximum or minimum value, and at a set distance from the surface, it reaches the main stream temperature. This distance signifies the thermal boundary layer [8].

The hydrodynamic and thermal fields interact and are interdependent in most cases. The thermal boundary layer will, however, be stronger for air flowing over structures. Conduction is the primary mode of heat transfer across the laminar zone of the boundary layer for a continuous surface. As a result of the thinner region and more mixing of the air layers in turbulent flow, the energy distribution is more pronounced than with laminar flow [8].

Another point to consider is the convective heat transfer coefficients (CHTC). CHTCs are commonly used to account for convective heat transmission. These CHTCs relate the convective heat flux normal to the wall q_{cw} (W/m^2) to the difference between the surface temperature at the wall T_w ($^{\circ}C$) and a reference temperature T_{ref} ($^{\circ}C$), it is commonly referred to as the temperature of the outside air. The convective heat flow away from the wall is believed to be positive [5].

The CHTC (W/m^2k) is defined as:

$$CHTC = \frac{q_{c,w}}{(T_w - T_{ref})} \quad (2)$$

These coefficients could be obtained by correlations or by means of CFD [5].

Finally, it should be mentioned the heat transfer rate from the solid surface, that is [12]:

$$q_{cv} = h_c A (t_w - t_f) \quad (3)$$

where h_c is the convection heat transfer coefficient which would be obtained from correlations in Section 4.

Finally, Equation 3 is not going to be developed, because as Reynolds and Nusselt number are going to be studied and will be defined later in Section 4, there is only the need of obtaining the h_c , and with this equation is not possible since it is not known what is the value of q_{cv} . The process of obtaining this dimensionless number is seen in Section 4.

4 Configuration in the wind tunnel

The case building is a small box ($15\text{cm} \times 15\text{cm} \times 15\text{cm}$) with a hole which is used to place a light bulb inside. It is attached to a table and this table is placed on the wind tunnel. The table has a hole shaped like a circle, the box is hooked to this and this can rotate, which is necessary to change the angle of the box.

The first experiment that was carried out was to see how the temperature in the design of the building rises rapidly. At first, it was seen that if we analyzed a larger box, reaching to the stable temperature (without the presence of air) was very hard, it was not even reached, and therefore it would take much longer to accomplish all the experiments, and therefore it was considered impractical.

An important fact that was considered was that reaching to the steady temperature once the light bulb is present had to be rapid (more or less about fifteen minutes). This was essential because having to make so many cases would take too much time to complete the measurements.

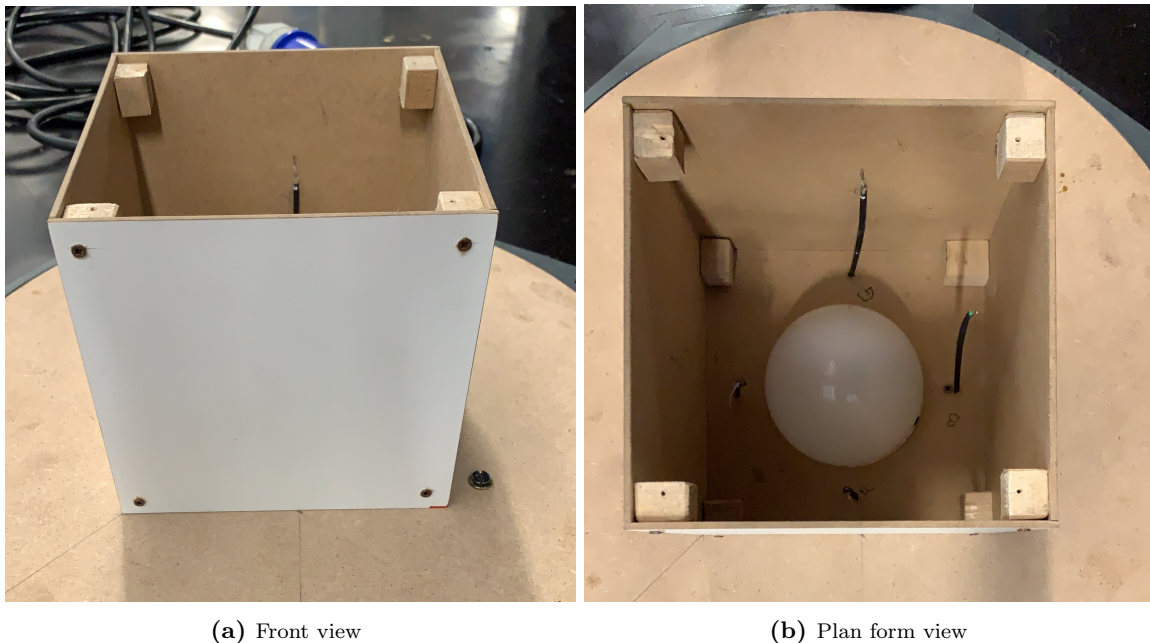


Figure 1: Configuration of the building case

The heat transfer is going to be evaluated with an Optris Infrared camera, Figure 2. Some of the advantages of the PI Precision Line are [13]:

- Interchangeable lenses
- Suited for fast processes (up to 1kHz)
- High thermal sensitivity (down to 40mK NETD)
- High optical resolution (up to 640×480 pixels)
- Laser blocking filter
- Temperature measuring ranges from -20 to $2000\text{ }^\circ\text{C}$
- Different spectral ranges ($500\text{nm}/1\mu\text{m}/7.9\mu\text{m}/7.5\text{--}13\mu\text{m}$)



Figure 2: Optris PI 400i camera [13]

This camera will take photos every second for thirty minutes. At the same time, a data logger with 4 thermocouples are placed inside the case building and so the difference in temperature inside the camera is also going to be analyzed, Figure 4. These thermocouples can be seen in Figure 1b. They are all placed at the same distance from the heat source both horizontally and vertically, as it can be seen in Figure 3.

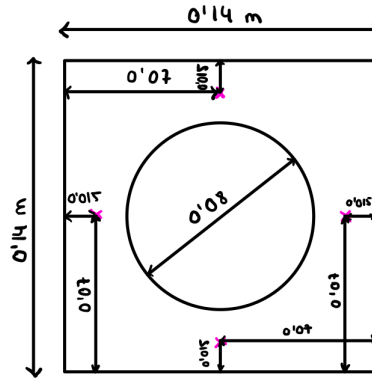


Figure 3: Location of the wires

It should be pointed out that there would be a difference between the temperature that shows the camera and the one taken out from the data logger. This difference in temperature will be what will be analyzed and is due to the difference between the temperature inside the sample building and outside in the presence of the wind.



Figure 4: Data logger configuration

As the table is uncovered, to avoid to the maximum the entrance of air by the front of the table, and that does not cool more quickly the box, a cover of Plexiglas has been anchored to the table.

So, the final configuration of the building case in the wind tunnel is seen in the Figure 5.

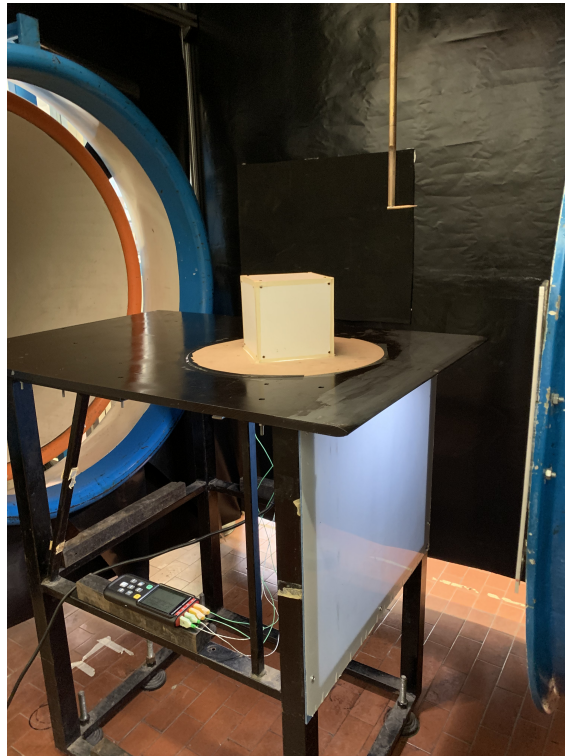


Figure 5: Final configuration of the building case in the wind tunnel

The cases that are going to be analyzed are with three different velocities, 5 m/s, 10 m/s and 15 m/s. The faces that will be analyzed in the orthogonal case will be: windward, leeward and parallel left. Moreover, 45 degrees of the building in the windward and leeward directions will also be computed. So, in Table 1

are the fifteen cases that will be analyzed.

Case	Velocity m/s
Orthogonal windward	5
Orthogonal windward	10
Orthogonal windward	15
Orthogonal leeward	5
Orthogonal leeward	10
Orthogonal leeward	15
Parallel left face	5
Parallel left face	10
Parallel left face	15
45 degrees windward	5
45 degrees windward	10
45 degrees windward	15
45 degrees leeward	5
45 degrees leeward	10
45 degrees leeward	15

Table 1: The cases that are going to be studied

The speeds chosen to make the analysis was not an easy task. Some factors have been taken into account.

Firstly, Reynolds number plays an important role in the determination of the different speeds. The ratio of inertial forces to viscous forces is known as the Reynolds number. This ratio distinguishes between laminar and turbulent flows [14].

Inertial forces resist a change in the velocity of an object and are the cause of the fluid movement. In turbulent flows, these forces are dominating. Otherwise, the flow is laminar if viscous forces, which are defined as resistance to flow, are dominating. The Reynolds number can be expressed in the following way:

$$Re = \frac{\textit{inertial force}}{\textit{viscous force}} = \frac{\rho V L}{\mu} = \frac{V L}{\nu} \quad (4)$$

where ρ (kg/m^3) is the density of the fluid, V (m/s) is the characteristic velocity of the fluid, L (m) is the characteristic length scale of flow, μ ($Pa \cdot s$) is the dynamic viscosity of fluid and ν (m^2/s) is the kinematic viscosity.

As can be seen in the Reynolds definition, the speed and the characteristic length are directly proportional. Therefore, as in this study the cube is reduced in comparison to a normal house, then the characteristic length is reduced and so the speed should be increased in order to have a similar Reynolds number, so a similar dynamic between the model and the real building. After reading articles analyzing a similar case, it has been possible to distinguish between two cases.

- The lower Reynolds number ranged between 2000 and 5000. As seen in [15] "Most of the available high-resolution wind-tunnel data of CHTC are based on measurements at relatively low Reynolds numbers 10^3 ".
- The Reynolds numbers analyzed are 3.1×10^4 , 5.8×10^4 , 8.2×10^4 and then 1.1×10^5 .

It has been established that the real case Reynolds number is 2.74×10^6 , it will be seen in Table 5 and Table 6.

Firstly, to have the Reynolds number in the first category, as it can be seen from the Table 2 ,the velocity should be between 0.2 (m/s) and 0.5 (m/s), which is not possible to set these velocities in the wind tunnel.

Reynolds	2.00×10^3	3.00×10^3	4.00×10^3	5.00×10^3
Characteristic Length (m)	0.15	0.15	0.15	0.15
Velocity (m/s)	0.21	0.31	0.42	0.52
Viscosity at 25°C (m^2/s)	1.57×10^{-5}	1.57×10^{-5}	1.57×10^{-5}	1.57×10^{-5}

Table 2: Reynolds number model case 1

Secondly, to be in the numbers of the second case, it can be observed the following table:

Reynolds	3.10×10^4	5.80×10^4	8.20×10^4	1.10×10^5
Characteristic Length (m)	0.15	0.15	0.15	0.15
Velocity (m/s)	3.24	6.07	8.58	11.51
Viscosity at 25°C (m^2/s)	1.57×10^{-5}	1.57×10^{-5}	1.57×10^{-5}	1.57×10^{-5}

Table 3: Reynolds number model case 2

Then, to analyze similar cases finally opted to analyze with the speeds already mentioned, so:

Reynolds	4.78×10^4	9.55×10^4	1.43×10^5
Characteristic Length (m)	0.15	0.15	0.15
Velocity (m/s)	5.00	10.00	15.00
Viscosity at 25°C (m^2/s)	1.57×10^{-5}	1.57×10^{-5}	1.57×10^{-5}

Table 4: Reynolds number cases analyzed

As it can be seen there is not a Reynolds number lower than 10^4 and there is not any higher than 10^5 .

However, just analyzing the Reynolds number is not enough because it should be considered a dimensionless number that takes into account heat transfer.

Through dimensional analysis, it is possible to demonstrate the existence of a functional relationship such that,

$$Nu = f(Re, Pr, Gr) \quad (5)$$

where, Nu is the Nusselt number, Re is the Reynolds Number, Pr is the Prandtl Number, and Gr is the Grashof Number [16].

The Nusselt number is an important metric that can help improve heat exchange rates. When discussing forced convection, the gravitational effects are usually insignificant in contrast to the forced velocity, hence the Grashof Number in the general equation can be ignored [8].

$$Nu = F(Re, Pr) = C(Re)^m(Pr)^n = \frac{hD}{k} \quad (6)$$

h is the heat transfer coefficient (W/m^2k), D is the inner diameter of the cube (m) and k is the thermal conductivity of the air (W/mK).

If the Nusselt number is close to 1, the heat transmission is solely conduction; however, if the value is between 1 and 10, the slug flow is laminar. It's active convection with turbulence in the 100–1000 range

if the range is greater. On the other hand, the Nusselt number is a non-dimensional heat transport coefficient. It's used to figure out whether heat is transferred through conduction or convection [16].

If there is no forced velocity in natural convection, the Reynolds number disappears from the equation.

$$Nu = F(Gr, Pr) = Constant(Pr)^x(Gr)^y \quad (7)$$

However, in the current studies, forced convection is present. The wind effect, such as the Reynolds number, is involved in the forced convection heat transfer process. When discussing forced convection, as mentioned before, the Grashof Number in the general equation can be ignored [8]. As a result, the functional connection is:

$$Nu_x = F(Re, Pr) = aRe_x^b Pr^c \quad (8)$$

where a , b and c are empirical parameters, Nu_x is the Nusselt number, based on the distance along the plate ($x - m$), Pr is the Prandtl number of air and Re_x is the Reynolds number, based on x and U_∞ [17].

Other flat-plate correlations were based on convective heat transfer tests on flat plates in wind tunnels, allowing empirical $CHTC - U_\infty$ correlations to be determined directly. Jürges' correlations, in particular, have been widely utilised in construction applications [17].

$$h_{c,e} = 4.0U_\infty + 5.6 \rightarrow U_\infty < 5m/s \quad (9)$$

$$h_{c,e} = 7.1U_\infty^{0.78} \rightarrow U_\infty > 5m/s \quad (10)$$

At low speeds, Jürges discovered a linear correlation that included buoyancy effects, as well as a power-law correlation for forced convection.

So, as the Reynolds number is suitable for the fluid dynamical conditions, but not entirely for temperature, the parameter of the Nusselt number has been studied. And the scaling together with Reynolds number is going to be analyzed.

It is important to mention that pure conduction heat transport is represented by a Nusselt number of value one (zero). Laminar flow has a value between one (zero) and ten. With turbulent flow typically falling between 100 and 1000. A higher Nusselt number indicates more active convection [18].

It will be established that the average temperature at which all the measurements have been made is 25°C. The thermal conductivity of the air is $k = 0.02551 W/mK$. The Prandtl number is going to be $Pr = 0.7296$ [19].

The Nusselt number has been calculated in two ways, following the Formula 6, and by correlations [20].

If the flow is laminar:

$$Nu_x = 0.332Re_x^{1/2} Pr^{1/3} \quad (11)$$

$$Pr \geq 0.6 \quad (12)$$

If the flow is turbulent:

$$Nu_x = 0.0296Re_x^{4/5} Pr^{1/3} \quad (13)$$

$$0.6 \leq Pr \leq 60 \quad (14)$$

$$5 \times 10^5 \leq Re_x \leq 10^7 \quad (15)$$

So, in a real case experiment, where the characteristic length could be $10m$, the velocity of the air has been set as the maximum speed achieved in my city, Valencia, the past year.

As the velocity is lower than $5 (m/s)$, the $h_{c,e}$ is calculated from the Equation 9.

Velocity (m/s)	Characteristic length (m)	Viscosity at $25^\circ C$	$h_{c,e}$
4.3	10	1.57×10^{-5}	22.82

Table 5: Data from the real case study

As in this case the Reynolds number is higher than 5×10^5 , the flow is turbulent so in order to calculate the Nusselt number the correlation that is going to be used is from Equation 13.

Reynolds number	Nusselt number formula	Nusselt number correlation
2.74×10^6	8945.51	3768.01

Table 6: Reynolds and Nusselt number real case

In the cases analyzed in the wind tunnel, the velocity is higher than $5 (m/s)$, so the $h_{c,e}$ is calculated from the Equation 10.

Velocity (m/s)	Characteristic length (m)	Viscosity at $25^\circ C$	$h_{c,e}$
5	0.15	1.57×10^{-5}	24.91
10	0.15	1.57×10^{-5}	42.78
15	0.15	1.57×10^{-5}	58.70

Table 7: Data from the model case study

The Reynolds number in the cases studied is lower than 5×10^5 , so the flow is laminar and the correlation for obtaining the Nusselt number is Equation 11.

Velocity (m/s)	Reynolds number	Nusselt number formula	Nusselt number correlation
5	4.78×10^4	146.50	65.33
10	9.55×10^4	251.56	922.38
15	1.43×10^5	345.14	113.15

Table 8: Reynolds and Nusselt number model case

At first, it was thought that the best thing would be to leave the same Reynolds as the one analyzed in the real case. But if the Reynolds number remains invariant, and the characteristic length is reduced by 0.015 , the speed must increase greatly, and in this case it is not possible to set the wind speed specifically to $287 m/s$.

So to see if our analysis is valid, it can be analyzed by seeing if the ratio between the Reynolds number and the Nusselt number is approximately the same.

Velocity ratio (m/s)	Reynolds ratio	Nusselt formula ratio	Nusselt correlation ratio
5/4.3	0.017	0.017	0.017
10/4.3	0.035	0.028	0.025
15/4.3	0.052	0.039	0.030

Table 9: Comparison between Reynolds and Nusselt

In the case of 5 m/s , the ratio of the Reynolds number and the Nusselt number between the velocity of the air in the wind tunnel and the velocity of the air in a real condition is the same, so it could be concluded that in this case, this velocity is a good estimation of the reality.

The problem if the speed is increased is that as the Reynolds number is increased, this ratio is approaching to 1 but analyzing the Nusselt number does not increase as quickly as the Reynolds and so there is a bigger difference of the order of magnitude, therefore it is very complicated that both ratios are equal.

In the end, because of using correlations it is seen that the relation of $h_{c,e}$ is not linear and the scale of the real case with the model is not predictable.

How this ratio develops depending on the speed can be seen in the Section 10.

Also, in Figure 40 it is seen how the Nusselt number changes with the speed. Firstly, there is a gap if the correlation is taken into account, this happens when changing from laminar to turbulent. Secondly, using the Formula 6 it is seen that this one increases with speed, as it is directly proportional to the $h_{c,e}$ and therefore this one is directly proportional to the speed.

In Figure 41 it is seen the development of the Reynolds number. It is also plotted the point where the real case is located.

Part III

Results and comparisons

Results and comparisons

First of all, the following images show how the camera captures the images when the data is processed.

The most visual method is realized with a Matlab function called "contour". In this case the images are taken out of the case with 45 degrees to 5 m/s and the case of orthogonal windward at 10 m/s .

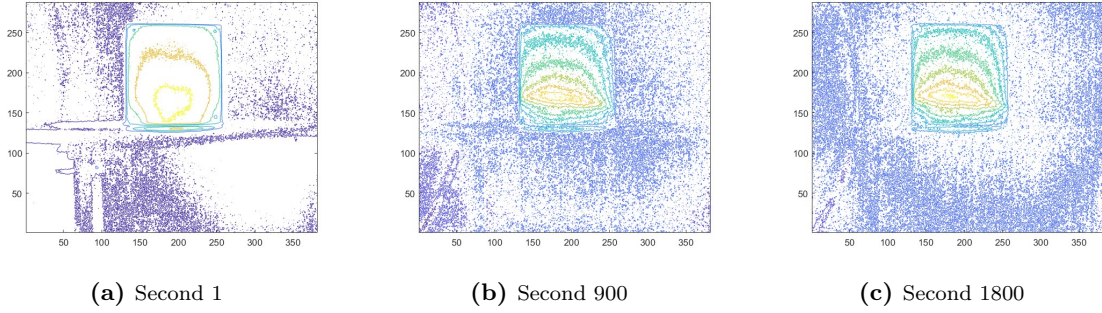


Figure 6: Contour 45 degrees windward at 5 m/s

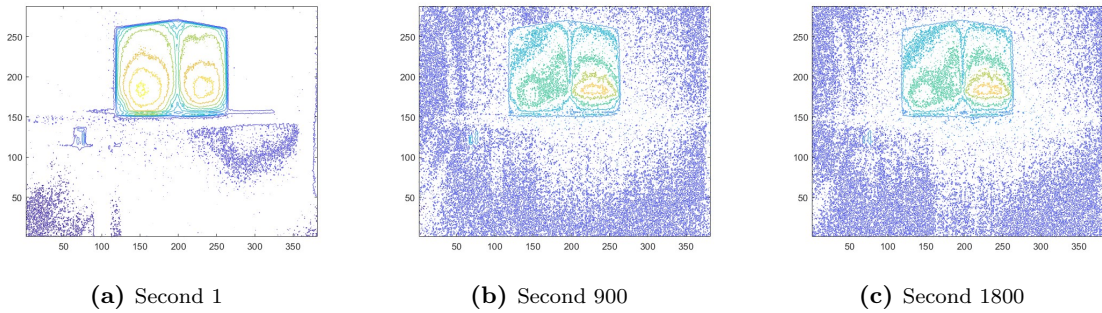


Figure 7: Contour orthogonal windward at 10 m/s

5 Parallel left face to the wind flow

5.1 Wind velocity of 5 m/s

As it can be seen in the Figure 8 the maximum temperature is 40.525°C and the minimum temperature is 34.325°C. The temperature becomes invariant 18 minutes after the experiment starts.

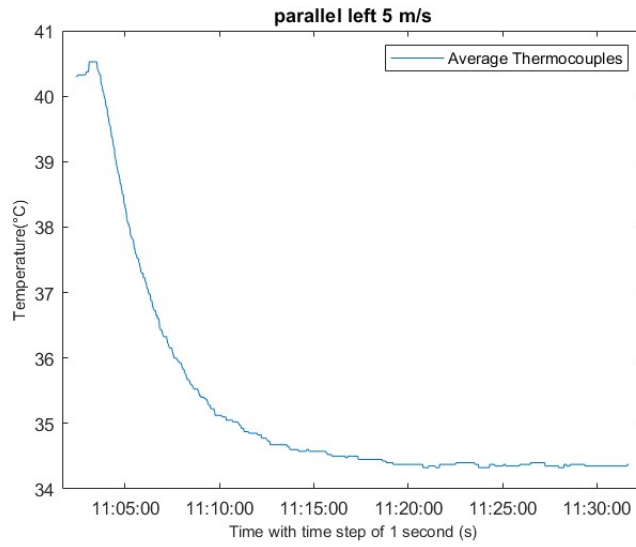


Figure 8: Data Logger test in the parallel left face at 5 m/s

In Figure 9 the maximum temperature is around 36°C, the mean maximum temperature of the points drawn is 34.40°C, the minimum is 27.634°C but the ambient temperature is lower, which moves around 26.80°C and 24.93°C.

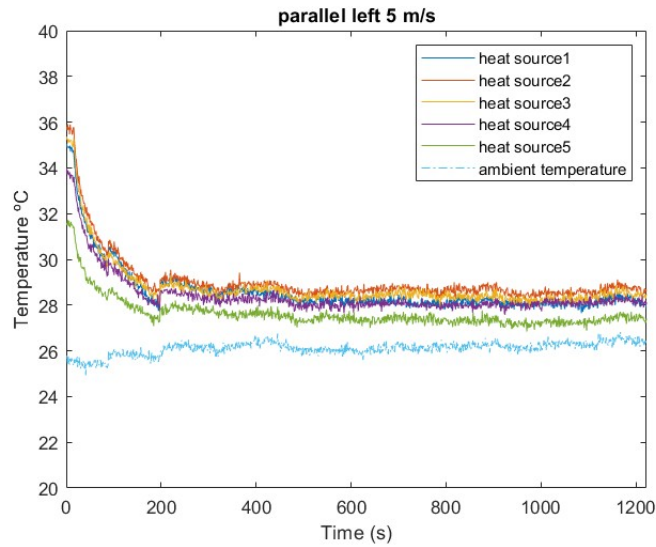


Figure 9: CSV processing data in the parallel left face at 5 m/s

5.2 Wind velocity of 10 m/s

Secondly, for 10 m/s the minimum temperature registered by the data logger is 28.435°C and the maximum temperature is 36.90°C. In this case the temperature becomes invariant around 12 minutes after starting the experiment.

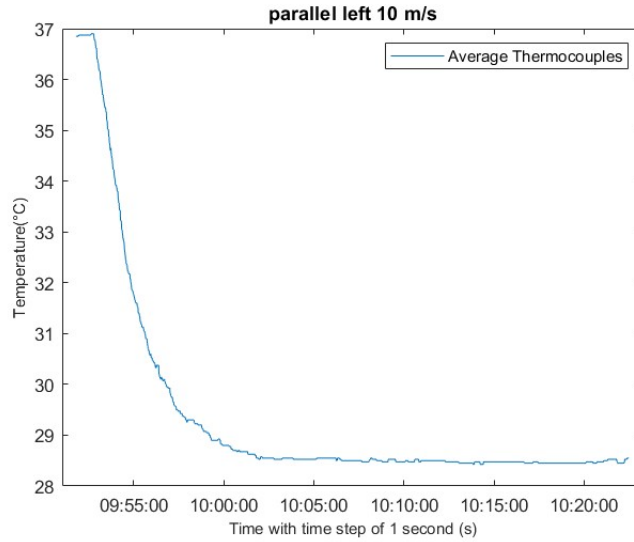


Figure 10: Data Logger test in the parallel left face at 10 m/s

In Figure 11 the maximum temperature is around 32.67°C, the mean maximum temperature of the points drawn is 31.44°C, the minimum is 24.16°C but the ambient temperature is lower, around 23.42°C.

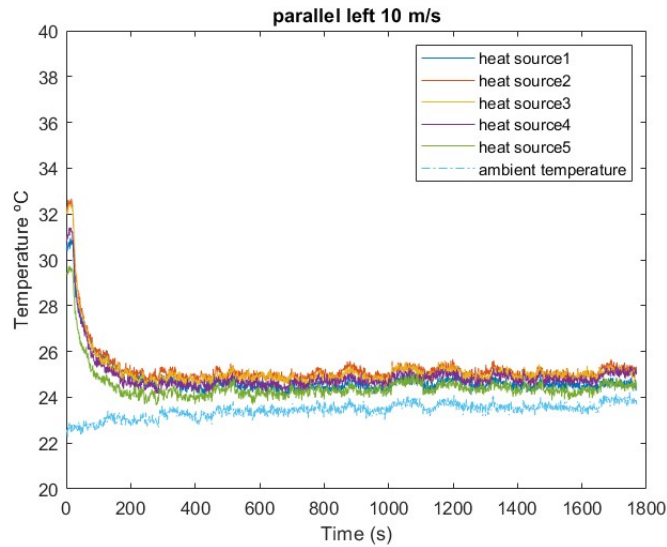


Figure 11: CSV processing data in the parallel left face at 10 m/s

5.3 Wind velocity of 15 m/s

The maximum temperature of the thermocouples is 38.70 °C and the minimum is 30.08°C. The temperature becomes invariant around 10 minutes after starting the experiment.

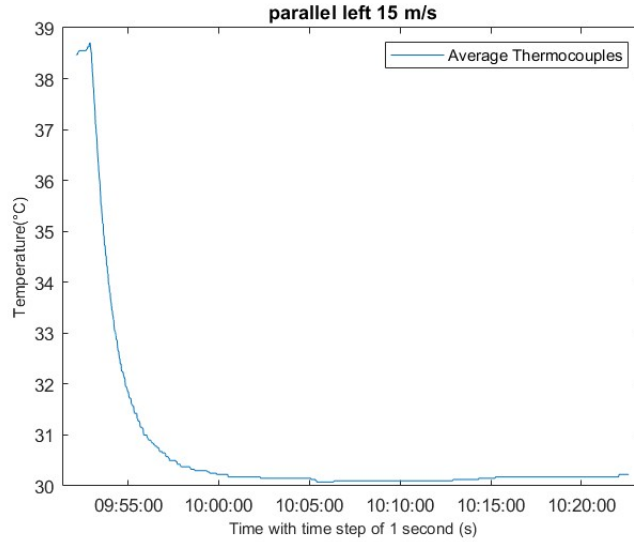


Figure 12: Data Logger test in the parallel left face at 15 m/s

The maximum temperature captured from the camera is around 35 °C, the mean maximum temperature is 31.35°C and the minimum around 26.47°C. The ambient temperature is around 26.58°C.

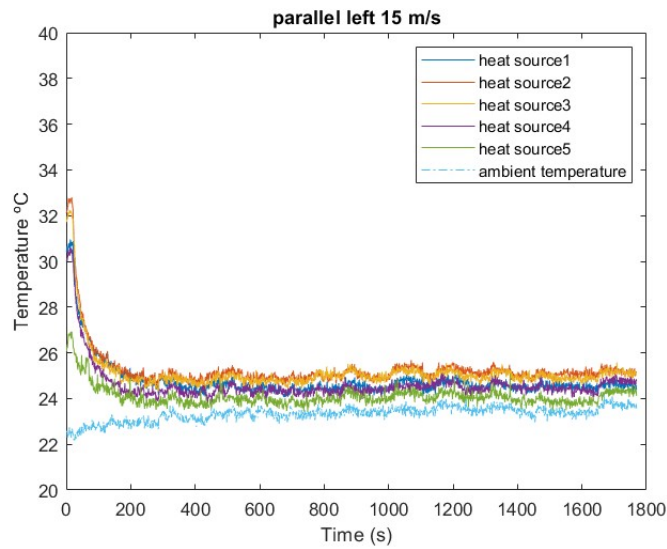


Figure 13: CSV processing data in the parallel left face at 15 m/s

6 Orthogonal windward

6.1 Wind velocity of 5 m/s

The maximum temperature reached by the data logger in this experiment is 38.48°C and the steady temperature is reached around 33.63°C. It could be mentioned that after 20 minutes of the beginning of the experiment the temperature becomes steady. In Figure 15 it is seen the highest temperature, which is 33.03°C. In average, the highest temperature in the cube is 31.80 °C, and the minimum is 26.90°C. The ambient temperature in this experiment is 25.43°C.

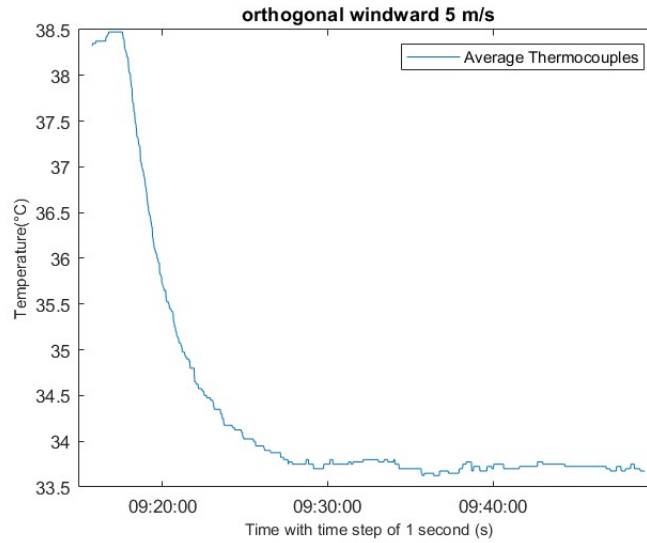


Figure 14: Data Logger test in the orthogonal windward at 5 m/s

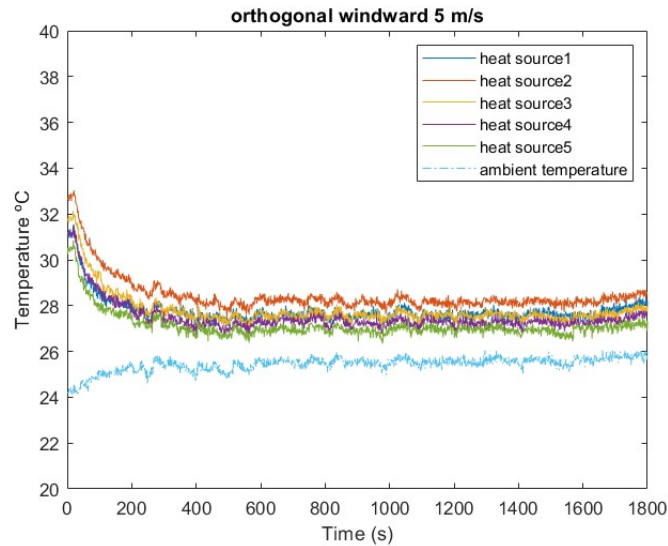


Figure 15: CSV processing data in the orthogonal windward at 5 m/s

6.2 Wind velocity of 10 m/s

The maximum temperature from inside the cube is 36.85°C until reaching the stability around 12 minutes after starting the study to a temperature of 28.70°C.

Regarding the temperatures captured by the camera, the mean maximum temperature in the cube is 30.94°C until arriving approximately to 25.11°C. The maximum temperature of the cube is 32.18°C. The ambient temperature of this experiment is 24.16°C.

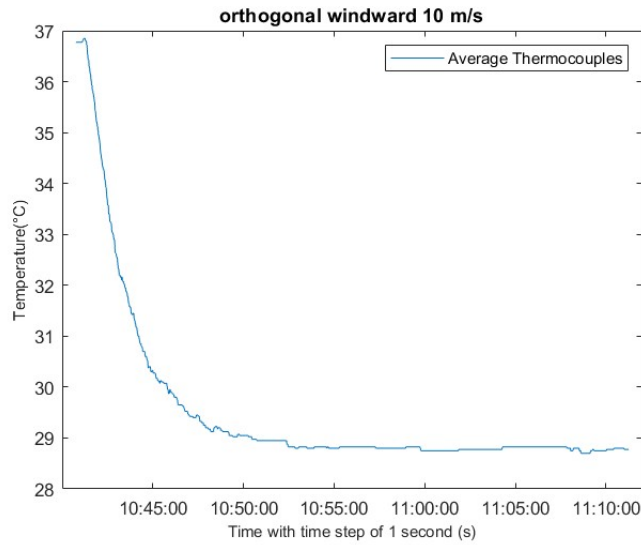


Figure 16: Data Logger test in the orthogonal windward at 10 m/s

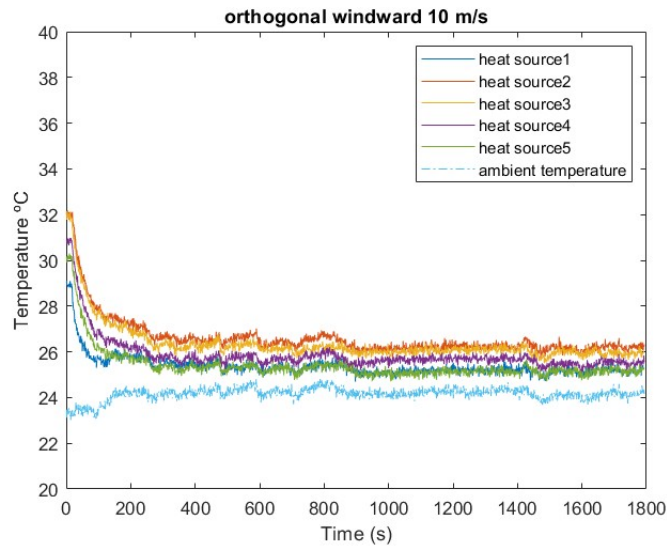


Figure 17: CSV processing data in the orthogonal windward at 10 m/s

6.3 Wind velocity of 15 m/s

Inside the cube the temperature is 38.60 °C when turning on the wind tunnel. It goes to 29.63 °C reaching its stability 9 minutes after starting.

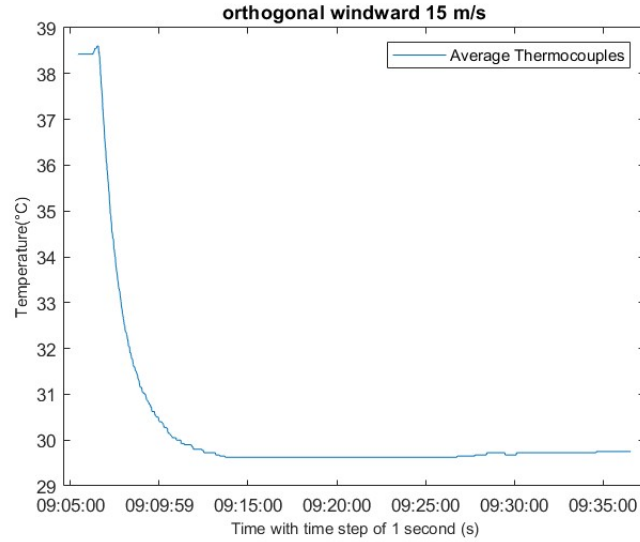


Figure 18: Data Logger test in the orthogonal windward at 15 m/s

The highest exterior temperature is 33.83°C. The mean maximum temperature is 32.76°C, until reaching equilibrium to 26.94°C.

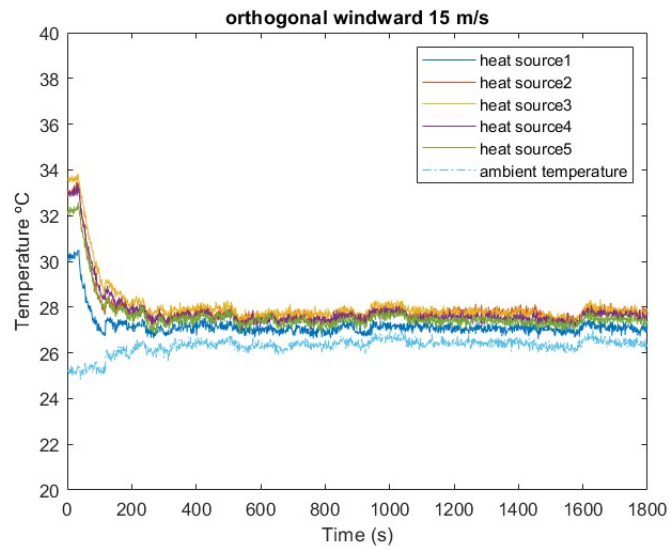


Figure 19: CSV processing data in the orthogonal windward at 15 m/s

7 Orthogonal leeward

7.1 Wind velocity of 5 m/s

In this case the time until reaching the steady state is 22 minutes. The experiment starts when the temperature is 38.80°C and goes to 34.225°C.

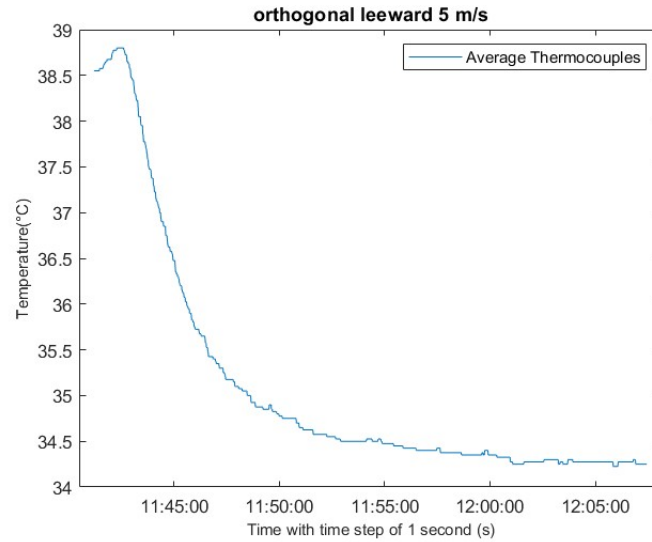


Figure 20: Data Logger test in the orthogonal leeward at 5 m/s

The maximum temperature that the infrared camera receives is 36.15°C, the mean of the maximum temperature of the points selected 35.12°C and the minimum 29.96°C, but the ambient temperature is even lower, 28.29°C.

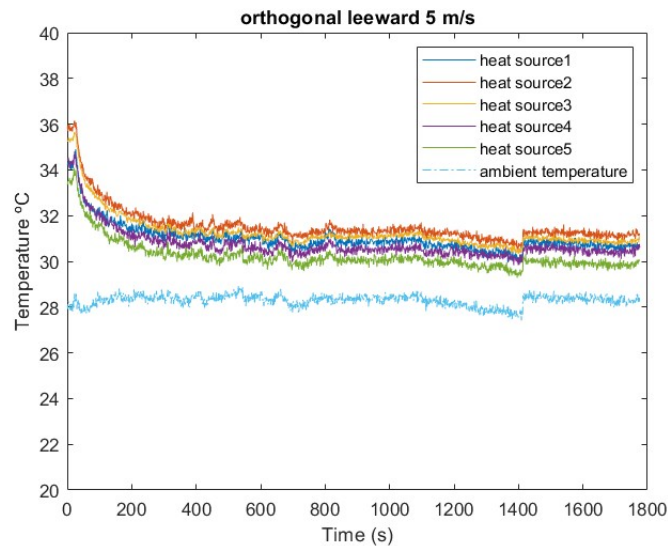


Figure 21: CSV processing data in the orthogonal leeward at 5 m/s

7.2 Wind velocity of 10 m/s

The data logger temperature goes from 36.68°C and arrives to 28.95°C after 14 minutes.

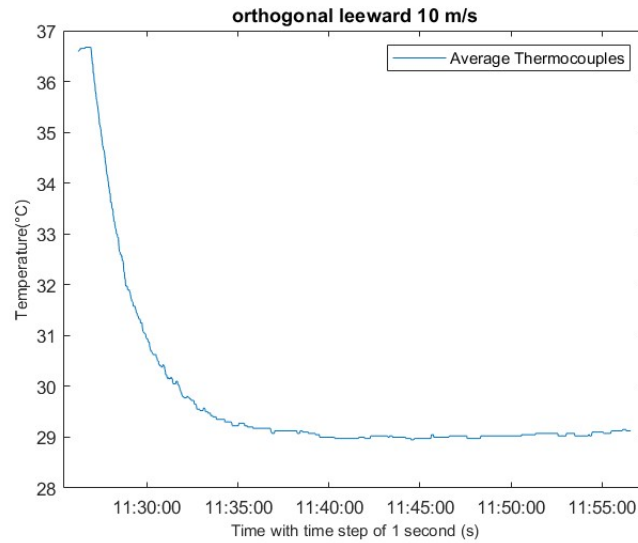


Figure 22: Data Logger test in the orthogonal leeward at 10 m/s

In Figure 23 the maximum temperature is 32.37°C, the temperature inside the cube at the beginning of the experiment is 31.37°C and approximately after 10 minutes is around 25.01°C . The ambient temperature is 23.92°C.

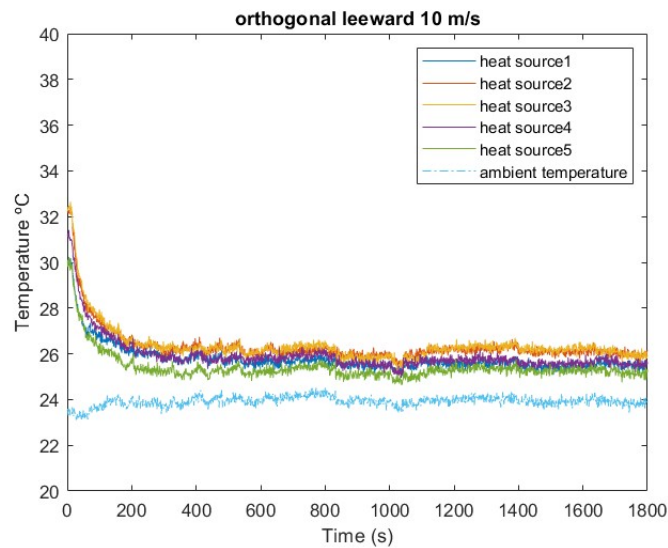


Figure 23: CSV processing data in the orthogonal leeward at 10 m/s

7.3 Wind velocity of 15 m/s

The maximum temperature is 38.80°C until reaching 30.45°C after 10 minutes.

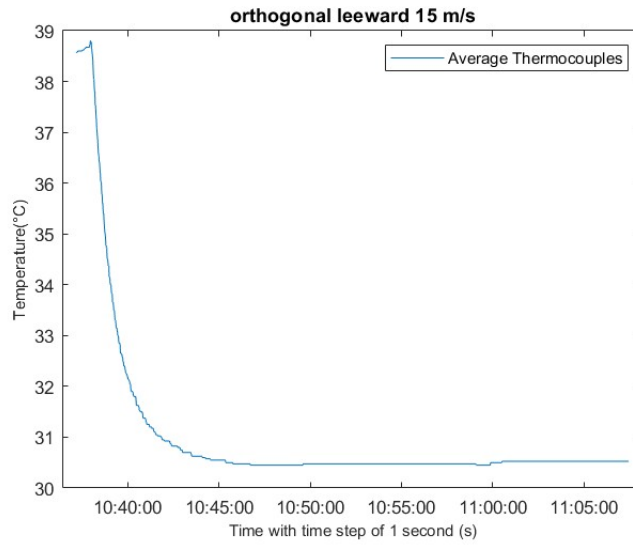


Figure 24: Data Logger test in the orthogonal leeward at 15 m/s

The maximum temperature of the points selected is 35.19°C. The maximum average temperature is 33.52°C, and the minimum is 27.67°C. The ambient temperature is 26.69°C.

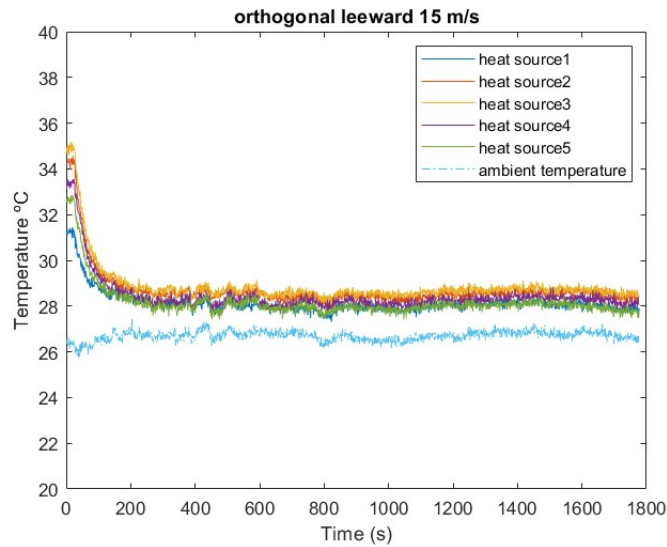


Figure 25: CSV processing data in the orthogonal leeward at 15 m/s

8 45 degrees windward

8.1 Wind velocity of 5 m/s

The attempt starts at a temperature of 39.23°C. In this case the temperature becomes constant 23 minutes after starting the experiment, reaching to a temperature of 31.13°C.

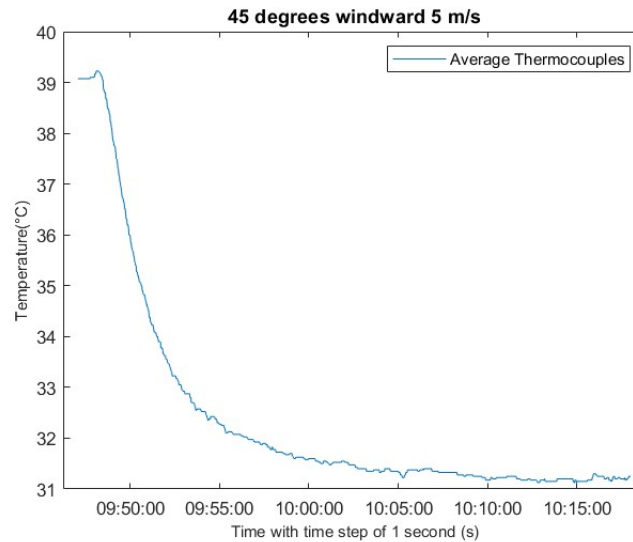


Figure 26: Data logger test in the 45 degrees windward at 5 m/s

In the case of the infrared camera, the maximum temperature that can be seen in Figure 27 is 34.56°C. The study starts approximately at 33.22°C and goes to 26.12°C. The ambient temperature in this case is 24.70°C.

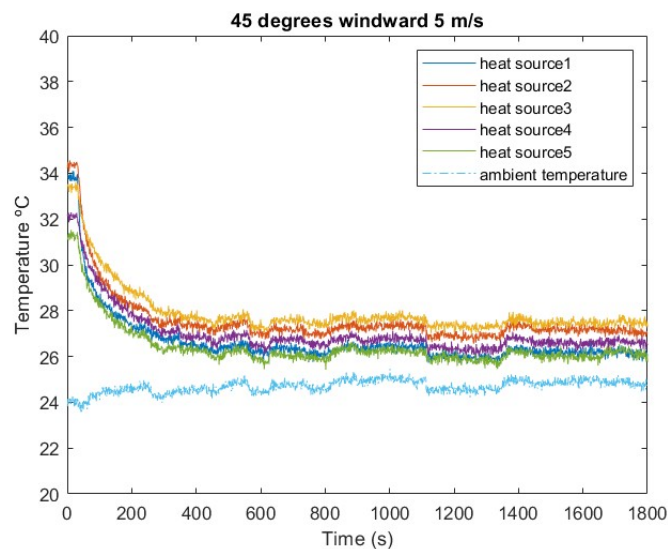


Figure 27: CSV processing data in the 45 degrees windward at 5 m/s

8.2 Wind velocity of 10 m/s

The maximum temperature taken by the thermocouples is 36.33°C and goes to 27.70°C 11 minutes after starting the probe.

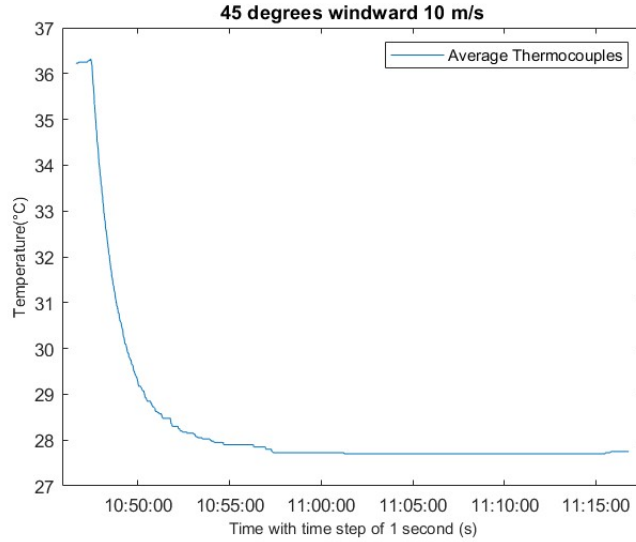


Figure 28: Data logger test in the 45 degrees windward at 10 m/s

The maximum temperature that can be seen in Figure 29 is 32.88°C. It goes from 31.44°C to 25.35°C and the ambient temperature is less, 24.28°C.

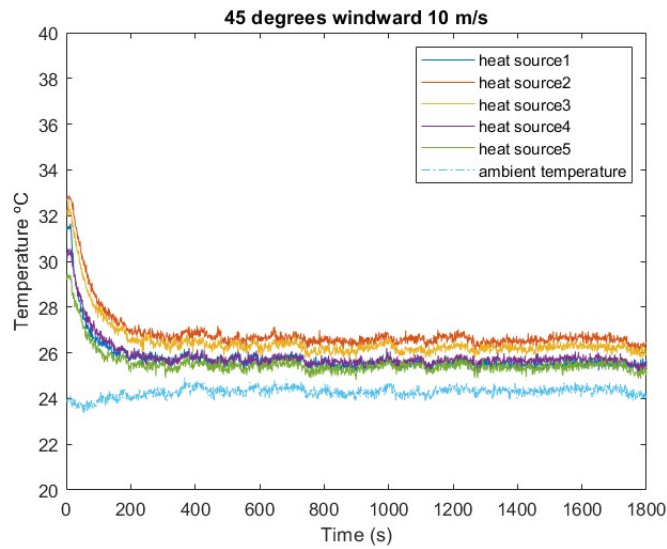


Figure 29: CSV processing data in the 45 degrees windward at 10 m/s

8.3 Wind velocity of 15 m/s

The temperature goes from 39.58°C until 30.90°C in 10 minutes.

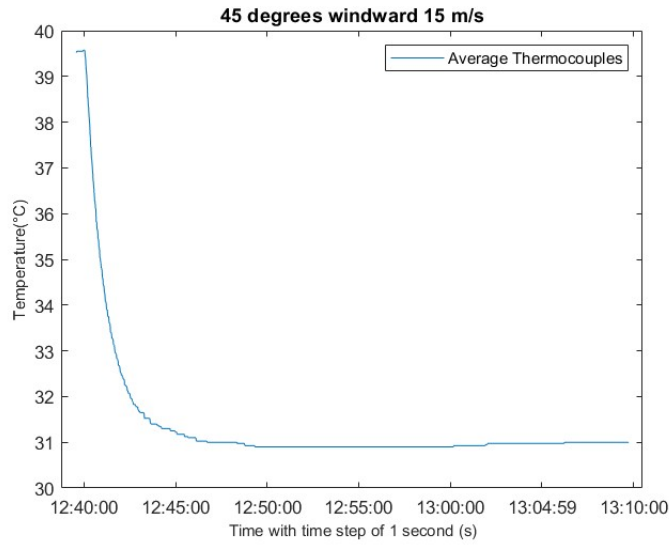


Figure 30: Data logger test in the 45 degrees windward at 15 m/s

The temperature captured by the camera goes from 34.01°C to 28.39°C in which the ambient temperature is 27.56°C.

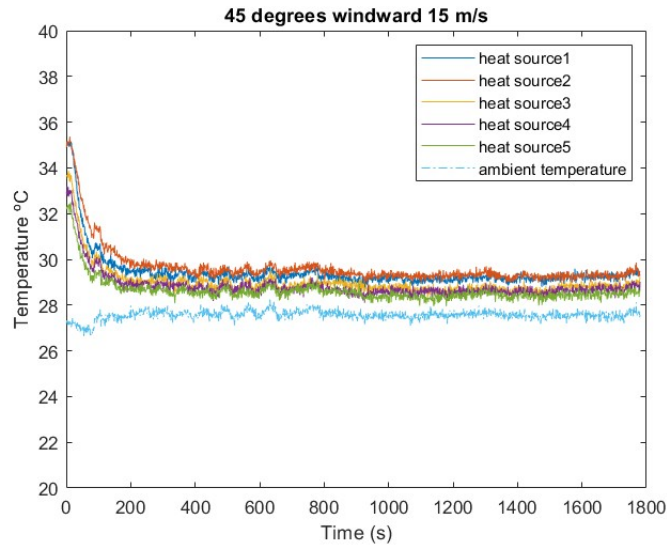


Figure 31: CSV processing data in the 45 degrees windward at 15 m/s

9 45 degrees leeward

9.1 Wind velocity of 5 m/s

In about 17 minutes the temperature descends from 39.00°C to 31.48°C.

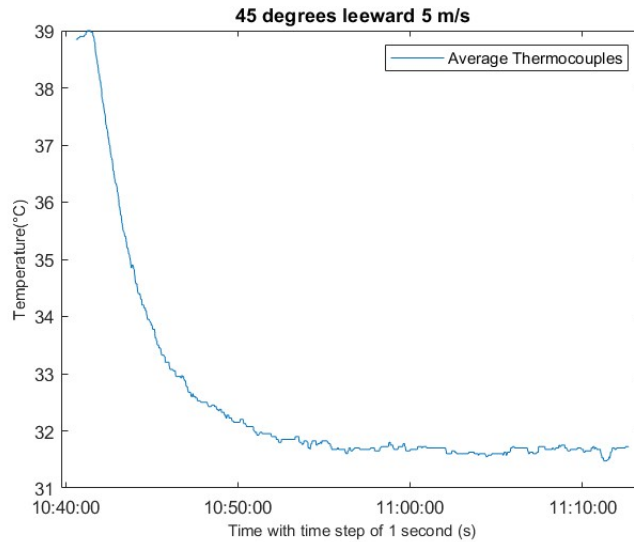


Figure 32: Data logger test in the 45 degrees leeward at 5 m/s

In this case the ambient temperature is 24.46°C but the temperature inside the cube goes just to 26.88°C coming from around 33.25°C.

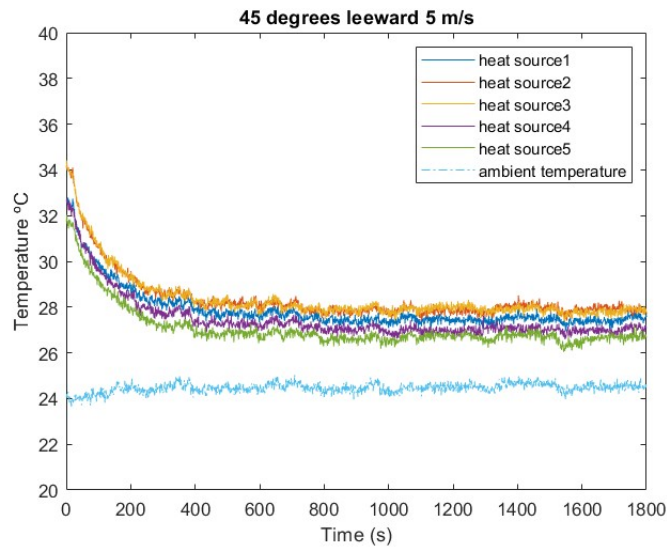


Figure 33: CSV processing data in the 45 degrees leeward at 5 m/s

9.2 Wind velocity of 10 m/s

In 11 minutes the temperature goes from 36.40°C until reaching the equilibrium to 27.45°C.

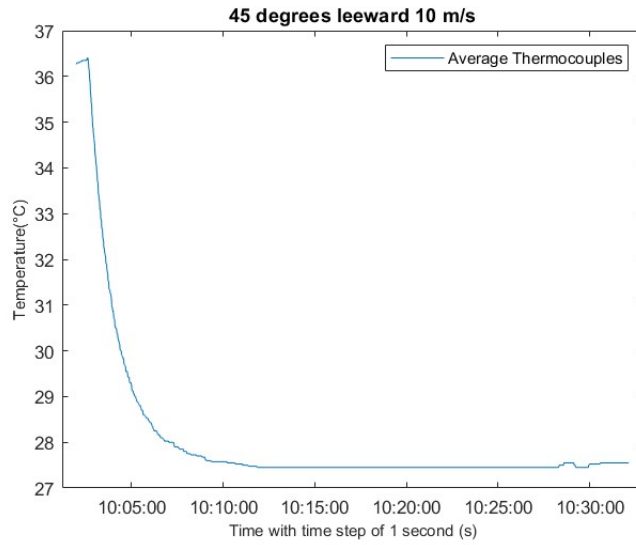


Figure 34: Data logger test in the 45 degrees leeward at 10 m/s

The maximum temperature in this case is 32.10°C, and the cube is at 24.23°C after 30 minutes. The ambient temperature is even lower, 23.45°C.

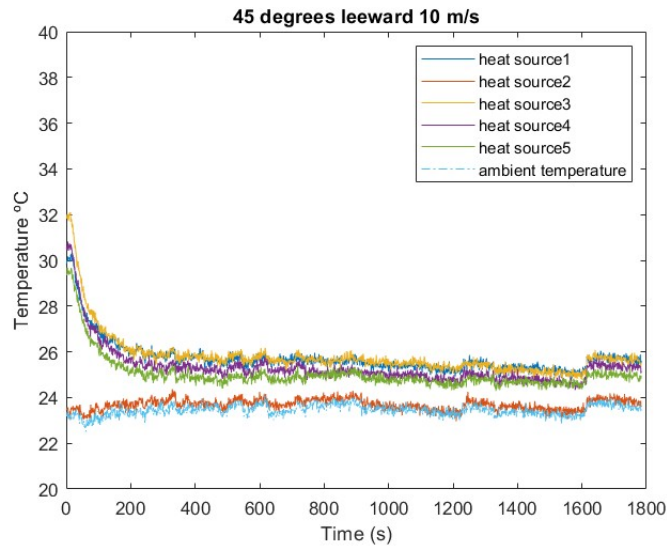


Figure 35: CSV processing data in the 45 degrees leeward at 10 m/s

9.3 Wind velocity of 15 m/s

In about 9 minutes the temperature becomes steady at 30.60°C and it starts at 39.13°C.

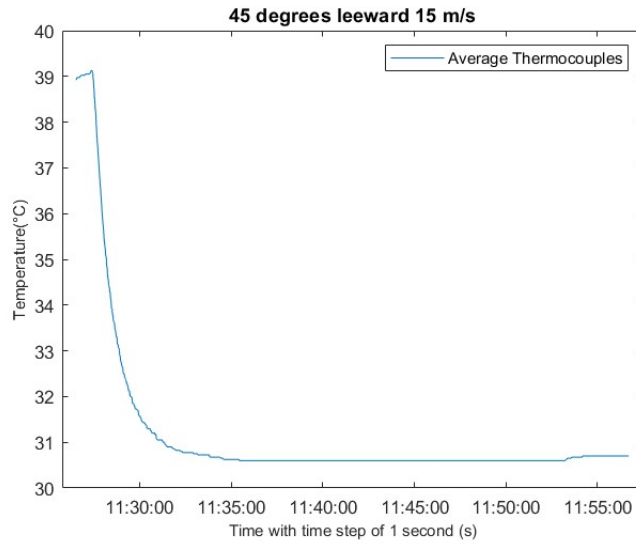


Figure 36: Data logger test in the 45 degrees leeward at 15 m/s

The ambient temperature in these measures is 27.08°C, but inside the cube is 28.08°C, coming from 33.86°C.

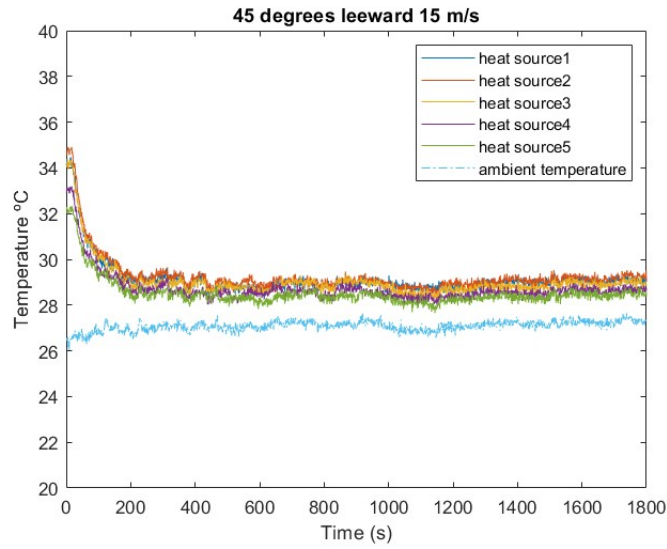


Figure 37: CSV processing data in the 45 degrees leeward at 15 m/s

Summary table

In Table 10 the resume of the temperatures is shown.

Case	Max. Temp. Datalog.	Max. Temp. Camera	Min. Temp. Datalog.	Min. Temp. Camera
Orth. windward 5	38.49	33.03	33.63	27.47
Orth. leeward 5	38.80	36.15	34.23	30.42
Orth. windward 10	36.85	32.18	28.70	25.74
Orth. leeward 10	36.68	32.65	28.95	25.12
Orth. windward 15	38.60	33.83	29.63	27.16
Orth. leeward 15	38.80	35.19	30.45	28.08
45 windward 5	39.23	34.56	31.13	26.56
45 leeward 5	39.00	34.41	31.48	27.39
45 windward 10	36.33	32.88	27.70	26.08
45 leeward 10	36.40	32.10	27.45	24.79
45 windward 15	39.58	35.36	30.90	28.91
45 leeward 15	39.13	34.90	34.33	28.30
Parallel left 5	40.53	35.91	30.08	28.18
Parallel left 10	36.90	32.67	28.44	24.57
Parallel left 15	38.70	35.04	30.08	27.25

Table 10: Summary of the temperature results

In Table 11 the difference between the temperature from the inside that was captured with the data logger and the temperature from the outside that was taken from the infrared camera is computed. It is clearly seen that the data logger shows a higher temperature than the camera. This is quite obvious as the thermocouples are closer to the heat source.

$$Diff.Max.Temp.\% = \frac{Max.Temp.Datalog. - Max.Temp.Camera}{Max.Temp.Datalog.} \times 100 \quad (16)$$

Case	Diff. Max. Temp.	Diff. Max. Temp. %
Orth. windward 5	5.46	14.19
Orth. leeward 5	2.65	6.83
Orth. windward 10	4.67	12.67
Orth. leeward 10	4.03	10.99
Orth. windward 15	4.77	12.36
Orth. leeward 15	3.61	9.30
45 windward 5	4.67	11.90
45 leeward 5	4.59	11.77
45 windward 10	3.45	9.50
45 leeward 10	4.3	11.81
45 windward 15	4.22	10.66
45 leeward 15	4.23	10.81
Parallel left 5	4.62	11.40
Parallel left 10	4.23	11.46
Parallel left 15	3.66	9.46

Table 11: Difference between temperature inside vs temperature outside

Another point to consider is the amplitude of each method used to measure the temperature. As it can be seen in Table 12, in almost all cases, the temperature measured from inside the box shows a greater difference between the maximum and the minimum temperature. This means that there is a bigger temperature jump, the slope of the drop is greater in the temperature measured from the inside.

One of the reasons why this can happen is because the camera was too far from the box, and it may be that the results are less accurate and do not capture the heat drop too well.

Case	Diff.Temp.Data logger	Diff. Temp. Camera
Orth. windward 5	4.86	5.56
Orth. leeward 5	4.57	5.73
Orth. windward 10	8.15	6.44
Orth. leeward 10	7.73	7.53
Orth. windward 15	8.97	6.67
Orth. leeward 15	8.35	7.11
45 windward 5	8.10	8.00
45 leeward 5	7.52	7.02
45 windward 10	8.63	6.8
45 leeward 10	8.95	7.31
45 windward 15	8.68	6.45
45 leeward 15	4.80	6.6
Parallel left 5	10.45	7.73
Parallel left 10	8.46	8.10
Parallel left 15	8.62	7.79

Table 12: The temperature amplitude of the data logger and the camera

10 Conclusions

After having carried out the work, it could be summed up with the conclusions obtained and possible improvements.

First of all, it is very important that no air enters the sample building, which means that the table should have been fully covered. But, if the table had been completely covered, it would not be possible to change the angle of the box. Also, the ability to insert the thermocouples and turn on the bulb would have been reduced.

Another aspect to mention is that sometimes the four thermocouples did not show exactly the same temperature when the wind tunnel was turned on. Being the difference between temperatures just over a degree, it was not given too much importance, and in the end all results have been obtained with the average of the four thermocouples for better results.

Another point to consider is that it should not be considered the temperature at which you start the experiment. This temperature varies depending on how long the heat source has been on until the experiment has been started and the wind tunnel has been aroused. Each time the experiment starts at a different temperature. Approximately, about fifteen minutes is the time needed to wait until reaching the temperature of equilibrium inside the cube, which is around 39.00 °C. But, the temperature of the outside air affects this temperature rise so it would not always be fifteen minutes until reaching the steady temperature.

It is also important to analyze the amplitude of the temperature, the difference between the maximum and the minimum temperature, and also until which temperature drops and stabilizes. That is to say, it has been observed that the temperature of the box never becomes the temperature of the air, then it can be said that the sample building is well isolated.

As we have seen analyzing the results, from inside the box, the temperature has a higher drop from the moment the wind tunnel is lit, and this drop is higher when more speed presents the wind tunnel. That is, when the wind speed is at 5 *m/s* it costs more to reach to the equilibrium temperature than when it is at 10 *m/s* and therefore when it is at 10 *m/s* it costs more than when it is at 15 *m/s*.

As it can be seen in Table 15, that is the summary of the minutes that it costs to reach the equilibrium inside the sample building, it is realised that as mentioned before, when having the lowest temperature is the hardest to reach balance. Also it is seen that when the angle is 90 degrees, it is harder reaching the steady state when been in the rear part of the sample building. However, when the angle is 45, in the windward is harder to reach to the equilibrium.

Regarding the temperatures, in all cases when analyzing the leeward, the temperature is higher than in the windward. This is because what first touches the air when it reaches the sample building is cooled before. This is a subject that should be mentioned, because when the first experiments were carried out, it was seen that if we saw the box from the side parallel to the flow, the part that was warmest was the part that was closest to the air stream. As it can be seen in the Section 10, in Figure 42, the temperature of four points of the right edge have been plotted. It is difficult to see any difference with Figure 9, but it is true that the minimum temperatures of the points from the edge are slightly higher. The minimum temperature of the points selected are seen in Table 17, and even the lowest temperature is still higher than the one seen in Table 10.

So, what happens in this study it can be seen in Figure 38. The stagnation points are in the orthogonal windward face, and because of this, re circulation occurs.

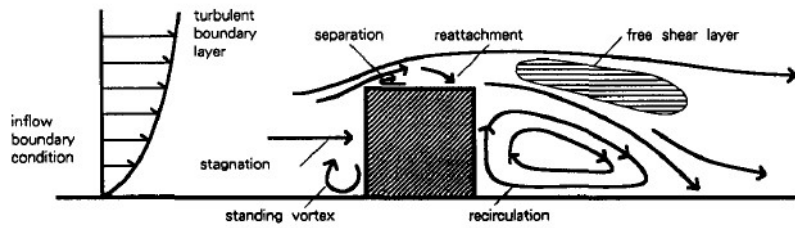


Figure 38: Flow field around a cube [21]

The following Figure is in the study made. It can be clearly seen how in the parallel face to the wind flow, there is more temperature in the right half of the face.

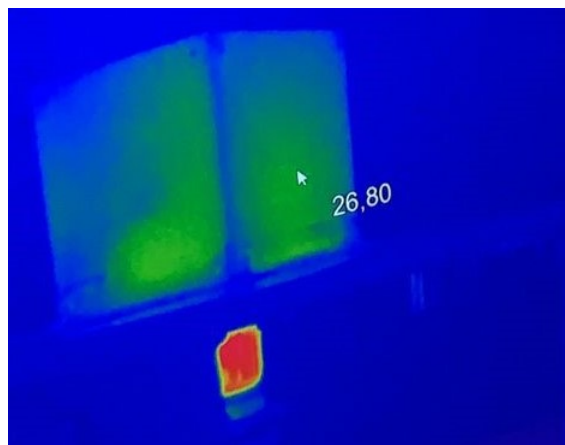


Figure 39: Flow field around a cube

As far as I am concerned, this point was good to be mentioned because was an important aerodynamic phenomenon that at first was not understood. This temperature difference is very small, not even it is of a degree, but as you can see in Figure 39 there is a contrast. This temperature difference shall be reduced as the speed increases. Finally, this can be seen in Figure 43 and Table 17, that these temperatures are approximately the same as seen in Figure 11.

References

- [1] James Oliver Smith. “Determination of the convective heat transfer coefficients from the surfaces of buildings within urban street canyons”. In: (2010). URL: <https://core.ac.uk/download/pdf/40038102.pdf>.
- [2] *Factors affecting electricity prices*. URL: <https://www.eia.gov/energyexplained/electricity/prices-and-factors-affecting-prices.php#:~:text=Changes%5C%20in%5C%20prices%5C%20generally%5C%20reflect,to%5C%20meet%5C%20the%5C%20increased%5C%20demand..>
- [3] *The new consumer: how new trends are shaping sustainability initiatives*. URL: <https://www.atlasrenewableenergy.com/el-nuevo-consumidor-como-las-nuevas-tendencias-estando-forma-a-las-iniciativas-de-sostenibilidad/>.
- [4] T.Stathopoulos and X.Zhu. “Wind pressures on buildings with appurtenances”. In: (1988).
- [5] Jan Carmeliet Thijs Defraeye. “A methodology to assess the influence of local wind conditions and building orientation on the convective heat transfer at building surfaces”. In: (2010).
- [6] D.J. Harris Y.Liu. “Full-scale measurements of convective coefficient on external surface of a low-rise building in sheltered conditions”. In: (2006).
- [7] D.L Loveday and A.H.Taki. “Convective heat transfer coefficients at a plane surface on a full-scale building facade”. In: (1995).
- [8] R.J.Cole and N.S Sturrock. “The convective heat exchange at the external surface of buildings”. In: (1977).
- [9] *Infrared technology, What is emissivity?* URL: <https://www.flukeprocessinstruments.com/en-us/service-and-support/knowledge-center/infrared-technology/what-emissivity%5C%3F>.
- [10] *Thermal Convection: Natural versus Forced Convection*. URL: <https://www.boydcorp.com/resources/resource-center/blog/thermal-convection-natural-versus-forced.html>.
- [11] M. Bahrami. “Forced Convection Heat Transfer”. In: (2011).
- [12] R Mark Rennie Peter Sutcliffe Alexander Vorobiev. “Control of Wind Tunnel Test Temperature Using a Mathematical Model”. In: (2013).
- [13] *Optris infrared cameras*. URL: <https://www.optris.global/infrared-cameras>.
- [14] *What is Reynolds number?* URL: <https://www.simscale.com/docs/simwiki/numerics-background/what-is-the-reynolds-number/>.
- [15] B. Blockena H. Montazeria. “Extension of generalized forced convective heat transfer coefficient expressions for isolated buildings taking into account oblique wind directions”. In: (2018).
- [16] *Nusselt Number*. URL: <https://www.sciencedirect.com/topics/chemical-engineering/nusselt-number>.
- [17] Jan Carmeliet Thijs Defraeye Bert Blocken. “Convective heat transfer coefficients for exterior building surfaces: Existing correlations and CFD modelling”. In: (2010).
- [18] *Nusselt number*. URL: https://en.wikipedia.org/wiki/Nusselt_number#:~:text=A%5C%20Nusselt%5C%20number%5C%20of%5C%20value,in%5C%20the%5C%20100%5C%E2%5C%80%5C%93100%5C%20range..
- [19] *Air - Thermal Conductivity vs. Temperature and Pressure*. URL: https://www.engineeringtoolbox.com/air-properties-viscosity-conductivity-heat-capacity-d_1509.html.

REFERENCES

- [20] McGraw-Hill Yunus A. Cengel. *Introduction to Thermodynamics and HeatTransfer, 2nd Edition*. 2008.
- [21] S. Murakami. "Comparison of various turbulence models applied to a bluff body". In: (1993).

Part IV

Annexes

Annex I

How speed change affects the Reynolds and the Nusselt number.

Velocity (m/s)	Reynolds number	Nusselt number formula	Nusselt number correlation
2	1.91E+04	71.97	41.32
3	2.87E+04	103.49	50.60
4	3.82E+04	127.01	58.43
5	4.78E+04	150.53	65.33
10	9.55E+04	251.56	92.38
15	1.43E+05	345.14	113.15
25	2.39E+05	514.08	146.07
35	3.34E+05	668.36	172.83
55	5.25E+05	950.87	1004.84
75	7.17E+05	1211.12	1287.82
95	9.08E+05	1456.34	1555.91
125	1.19E+06	1803.97	1937.91
150	1.43E+06	2079.65	2242.23
175	1.67E+06	2345.36	2536.51
200	1.91E+06	2602.81	2822.48
250	2.39E+06	3097.65	3374.11
287	2.74E+06	3449.75	3768.01

Table 13: Reynolds and Nusselt number model case

Velocity ratio (m/s)	Reynolds ratio	Nusselt formula ratio	Nusselt correlation ratio
2/4.3	0.007	0.009	0.011
3/4.3	0.010	0.012	0.013
4/4.3	0.014	0.014	0.016
5/4.3	0.017	0.017	0.017
10/4.3	0.035	0.028	0.025
15/4.3	0.052	0.039	0.030
25/4.3	0.087	0.057	0.039
35/4.3	0.122	0.075	0.046
55/4.3	0.192	0.106	0.267
75/4.3	0.261	0.135	0.342
95/4.3	0.331	0.163	0.413
125/4.3	0.436	0.202	0.514
150/4.3	0.523	0.232	0.595
175/4.3	0.610	0.262	0.673
200/4.3	0.697	0.291	0.749
250/4.3	0.871	0.346	0.895
287/4.3	1.000	0.386	1.000

Table 14: Comparison between Reynolds and Nusselt

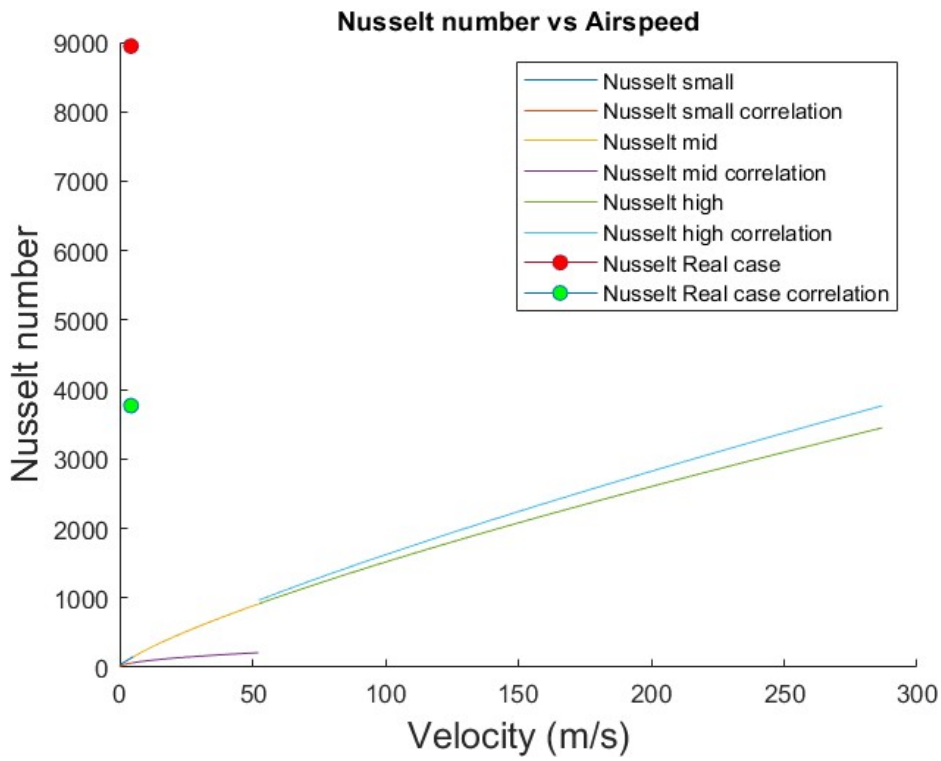


Figure 40: Nusselt number changing with the velocity of the air

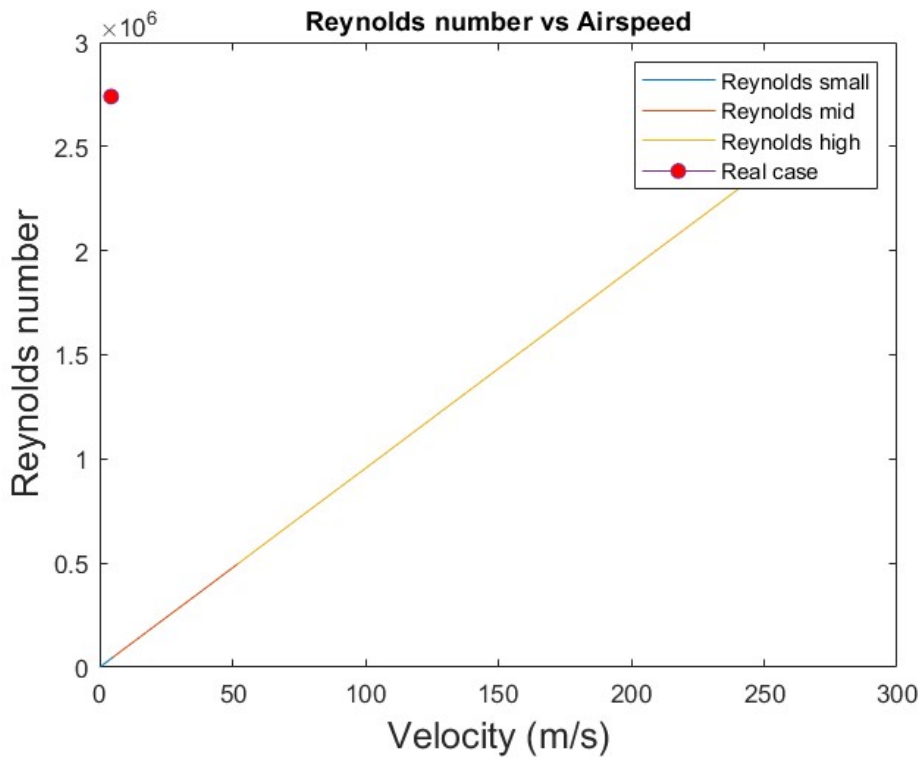


Figure 41: Reynolds number changing with the velocity of the air

In Figure 40 there is a distinction between the dimensionless number obtained from the correlations mentioned and the one obtained just substituting in the formula of the Nusselt number. It is separated in small, mid and high because the value of the $h_{c,e}$ changes with the different speeds and also the correlation between turbulent and laminar flow.

In Figure 41:

- Reynolds small means that the velocity is lower than 5 (m/s) and the Reynolds number is laminar.
- Reynolds mid means that the velocity is higher than 5 (m/s) and until the value of the velocity when the Reynolds become turbulent.
- Reynolds high goes from the from the speed at which the flow becomes turbulent.

Annex II

Summary of the results.

Case	Minutes
Orth. windward 5	20
Orth. leeward 5	22
Orth. windward 10	12
Orth. leeward 10	14
Orth. windward 15	9
Orth. leeward 15	10
45 windward 5	23
45 leeward 5	17
45 windward 10	11
45 leeward 10	11
45 windward 15	10
45 leeward 15	9
Parallel left 5	18
Parallel left 10	12
Parallel left 15	10

Table 15: Minutes to reach the equilibrium from inside the cube

Flow re circulation

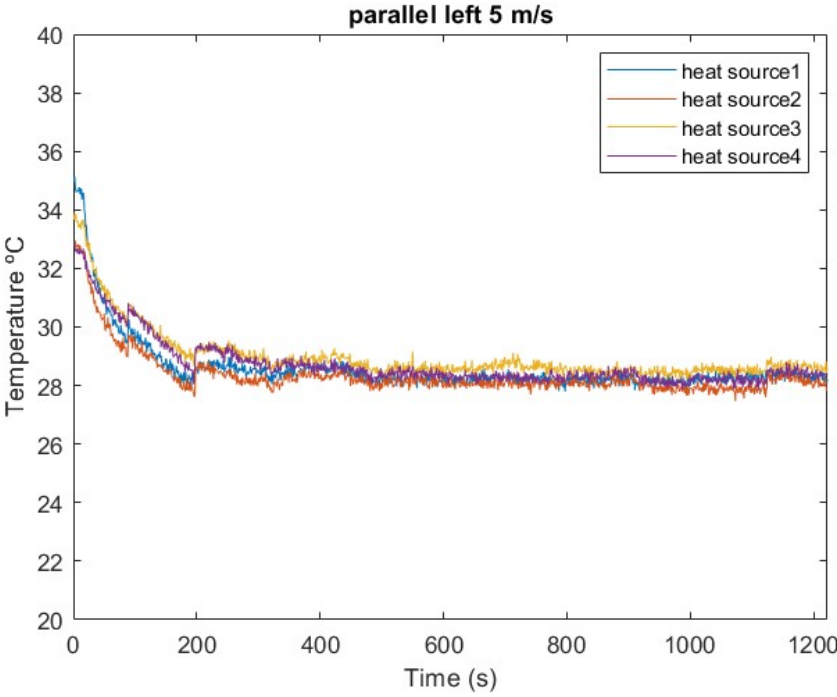


Figure 42: CSV processing data in the half right parallel left face at 5 m/s

Case	Minimum Temperature °C
Point 1	27.79
Point 2	27.47
Point 3	28.12
Point 4	27.83

Table 16: Minimum temperature of points from the right edge in 5 m/s

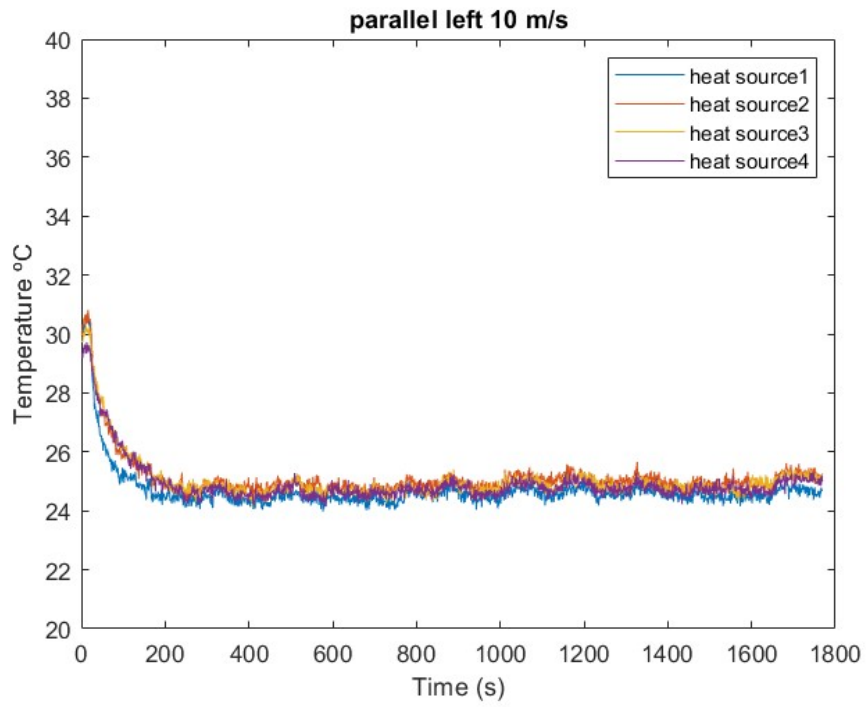


Figure 43: CSV processing data in the half right parallel left face at 10 m/s

Case	Minimum Temperature °C
Point 1	23.98
Point 2	24.27
Point 3	24.12
Point 4	24.16

Table 17: Minimum temperature of points from the right edge in 10 m/s